33RD CONGRESS
OF THE INTERNATIONAL COUNCIL
OF THE AERONAUTICAL SCIENCES
STOCKHOLM, SWEDEN, 4-9 SEPTEMBER, 2022

AERODYNAMIC INVESTIGATION OF VERY CLOSELY FLYING FIGHTERS TO DEVELOP NEW FORMATION TYPES

Süleyman Mert Aydın[1,2], Abdurrahman Gazi Yavuz[2] & Mustafa Kaya[1]

[1]Aerospace Engineering Department, Yildirim Beyazit University, Ankara 06010, Turkey
[2]Turkish Aerospace Industries, Ankara 06980, Turkey

Abstract

New generation fighters serve as game-changers in the operational environment within the scope of today's technological capabilities. In present, the old generation fighters have to fight against the 5th generation fighters. Considering the innovations in the new generation, in order to be successful in a fighting mission, apart from technological developments, the fighters need to diversify their performance levels, subsystem performances, and, most importantly, operational concepts. As part of performance capabilities and system capabilities for aircraft platforms, there are many different tactical formations implemented in the operational environment. These formations plan to maximize the performance of the aircraft from the operational perspective. This work covers the studies to strengthen the survivability and lethality factors for Friendly (Blue) Force platforms by using specific close flight formation sequences against the problems encountered in the detection and targeting algorithms of the Opponent (Red) Force fighters' own radar systems. For this purpose, the methods used for the aerodynamic analyses were first validated against the available DLR-F4 data. Then, F-16 single aerodynamic analyses were performed. The data obtained from these results were used for multiple analyses, and ideal formation sequences were determined. Aerodynamic analyses of 4th generation fighters in a very closely flying formation were performed using CFD methods for different triple and quadruple F-16 formation sequences, and the predicted studies reached the desired results. These results were interpreted with the perspective of Operational Analysis for the analysis of the effectiveness in the operational environment, and a new perspective was gained on the effectiveness of the old generation fighters in the operational environment.

Keywords: Applied Aerodynamics, Operational Analysis, Computational Fluid Dynamics (CFD), Close Formation, Radar Cross Section (RCS).

1. Introduction

Operational analysis is a perspective that aims to achieve maximum performance in a field where it will be used, specific to the project being studied, the system to be analysed and succeeded. Analysing the effectiveness of any platform planned to be produced in the defence industry in the operational environment concerns all stages, including the design criteria before production. Since years of the Second World War, countries are still using the operational analysis methods, which they used to analyse and determine the factors that will give them an advantage in the operational environment and develop them together with the changing technology. It is of great importance to develop the decision mechanism by evaluating all studies on a defence platform from an operational perspective together with technical analysis. For this reason, the results of all the analysis studies have done in this thesis will be blended with the operational analysis methods and will evolve into research that will serve in this sector.

Based on the study to be analysed, a real problem of the detection and targeting algorithm encountered in the airborne radar systems of Opponent (Red) Force fighters, is turned into an advantage for Blue Force by the use of the close flight concept by the F-16 Falcon C Model, which is accepted as the Friendly (Blue) Force 4th Generation Fighter. Although radar systems are very advanced systems within the framework of today's technological developments, they can detect and target from almost 50-100 Nm in Air-Air engagements. While they can show high performance in different weather conditions, they can have many features such as targeting more than one aircraft at the same time. Since these avionic mission systems used by multiple forces have very similar capabilities, they can achieve the difference that will lead them to success in the operational environment with many methods such as electronic countermeasure systems, low observability (LO), and tactical manoeuvres. However, according to previous operational environment experiences, Radar systems cannot perform target distribution for very close platforms that appear on the pilot's screen or can see the oncoming systems as a single platform with higher RCS, although they can use their detection capability when they encounter a trail, box and similar arm flight approaching them. This situation can increase both survivability and lethality for platforms which uses the close flight formation as it allows threat systems to approach and shoot at closer distances. At this point, it is important to conduct an aerodynamic analysis of 4^{th} generation fighters flying subsonic (up to 0.9 M) and flying overhead during the approach to air-air engagement. It is aimed to optimize the lateral distance and altitude difference that should be between them. The smaller these differences, the greater the advantage against the threat force's radar system.

The aerodynamic analysis of aircrafts flying very close to each other for developing new formation types in the operational environment is not a common topic in the literature. In this study, aerodynamic analyses were made to define the optimum distance at which triple and quadruple F-16s can fly close to each other using CFD methods. Thus, the formation type that provided the specified criteria and provided maximum benefit in the operational environment was determined at the end of the study. Examples of aerodynamic analysis studies for multiple flights are available in the literature [1]- [2]- [3]- [4]- [5]. The studies in the literature were examined for the methodology and planned to be applied for this study.

2. Methodology

2.1 Validation

At the beginning of the studies, validation processes were carried out in order to verify the use of CFD solver. German DLR-F4 Model aircraft is seen in Figure 1, which is frequently preferred in the literature for validation analyses.

A DLR-F4 Model, which is compatible with real measurements and suitable for CFD analysis, was obtained from open source, and the analysis was carried out in accordance with the analysis conditions in "AGARD Advisory Report No: 33" and verified with the analysis model created.

Analyses were performed at Standard Sea Level at 0.75 M with Reynolds Number of 3millions. The eddy viscosity is modelled using the SST k-ω (with wall function) turbulence model. Since there is a wall function, the y+ value is adjusted to be 30.

The CFD analyses were performed with using the commercial software ANSYS Fluent with a second-order accurate and upwind discretization of conservation equations. The turbulence equations were discretized using a first order upwind approximation.

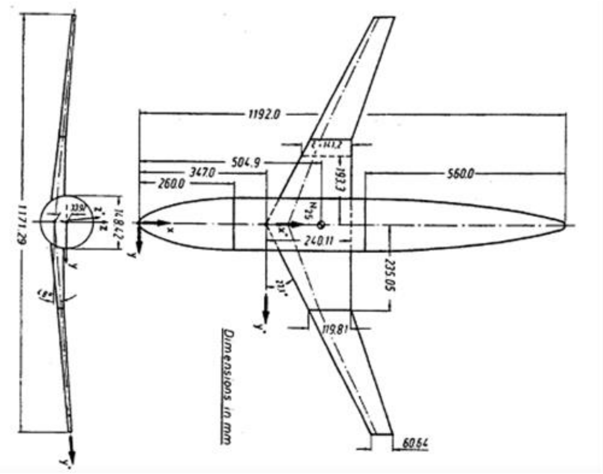

Figure 1-DLR-F4 Model dimensions [6]

Then, the analyses result of the DLR-F4 were compared with the results obtained from the relevant source and the similarities of the results between CFD solution and experimental results as in the Figure 2 were observed.

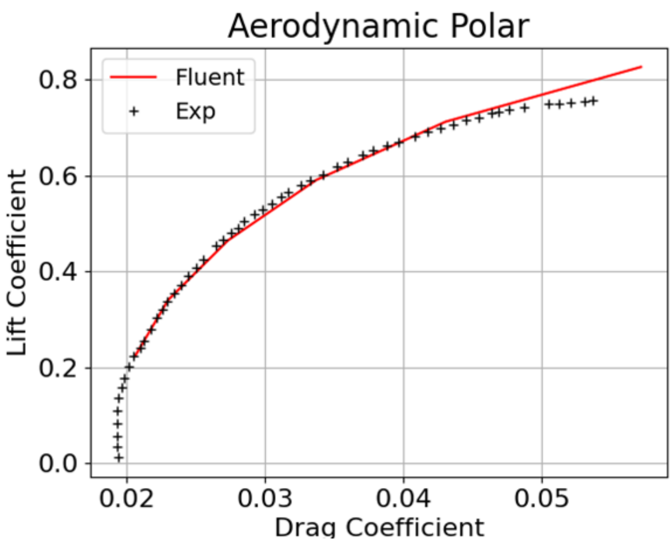

Figure 2- C_L vs C_D result comparison with experimental results of DLR-F4

2.2 Mesh Methods for Single F-16 and Formation Sequences

For the analysis, F-16 Fighting Falcon C model, was used. The model was cleaned using ANSYS SpaceClaim and made suitable for meshing. Mesh was made under the assumptions at the bottom using Pointwise software.

- Aircraft surface is discretized by Advancing Front Ortho method in Pointwise
- First wall distance is set to keep y+ value around 30
- Boundary Layer cells are created by T-rex algorithm to surround Aircraft surface
- Flow volume is discretized by Delaundo algorithm
- Approximately 25 of full layers are created

Figure 3-5 show some steps from the meshing process.

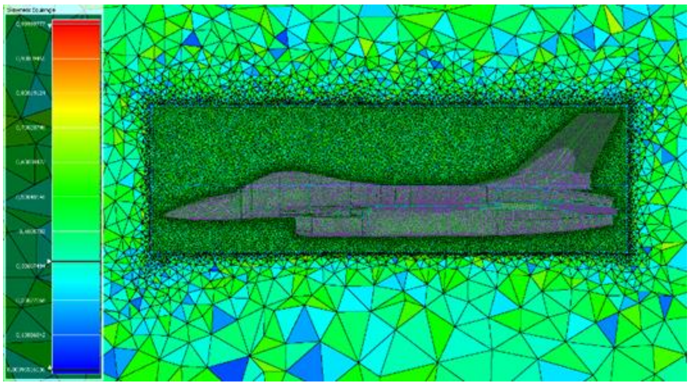

Figure 3-Single F-16 3D surface mesh

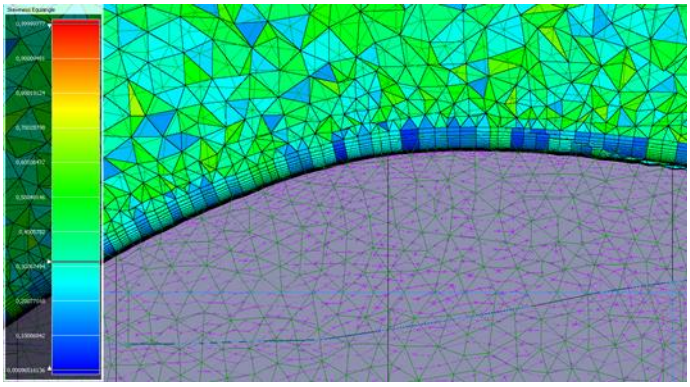

Figure 4-Single F-16 mesh layers around the surface

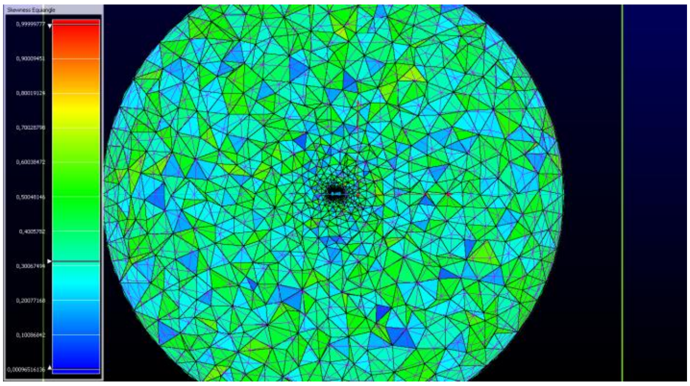

Figure 5-Single F-16 volume mesh

Table 1-Total cell number of mesh

Formation Type	***Total Cell Number***
Single F-16	6,228,351
Triple Formation Sequence	19,235,753
Quadruple Formation Sequence	25,638,139

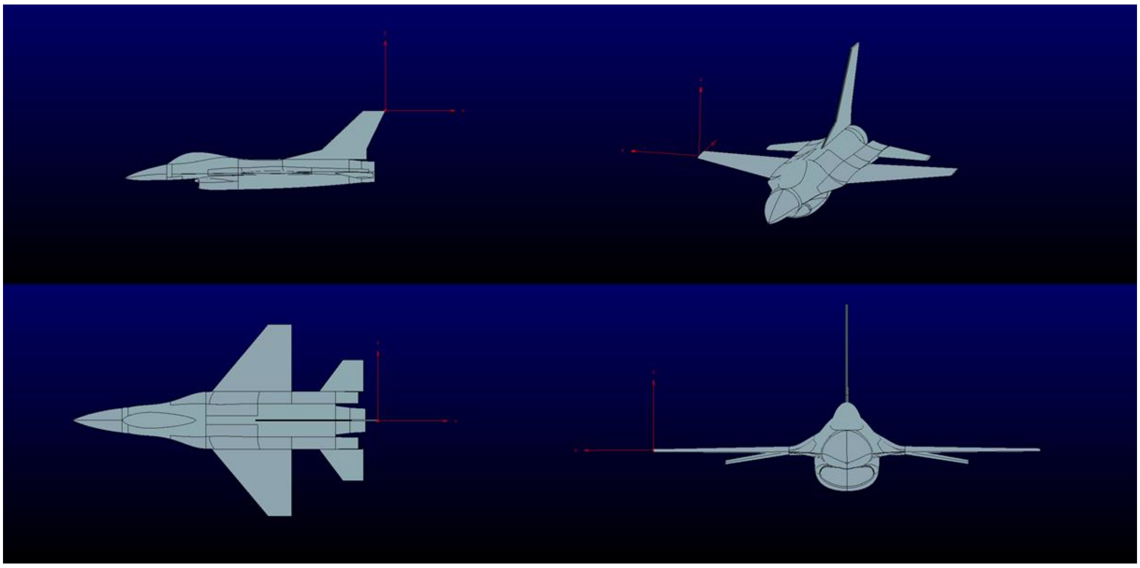

Figure 6-F-16 3D Model used for analyses

The block created on the geometry will contain a single F-16 geometry. When the block is validated, aerodynamic analysis can be performed for the desired formation type by positioning these blocks in space in a way that does not affect each other for formation sequences.

2.3 CFD Analyses for Single F-16

After the validation studies with the DLR-F4, single F-16 CFD analyses were performed on ANSYS Fluent at standard atmosphere sea level conditions with the freestream Mach Number of 0.9. The SST k-ω equations are used to model the turbulence for different aoa values as [-0.5, 0., 0.5, 1., 1.5]. Computations have been done in a parallel computing environment using 40 processors on HPC (High Power Computing).

2.3.1 Numerical Solutions

CFD solutions were performed with ANSYS Fluent which is well-known commercial analysis software which includes Navier-Stokes equations using method of finite volume on unstructured mesh for aerodynamic calculations of formation sequences.

$$\frac{\partial}{\partial t}\int_{A} U dA + \int_{A} \vec{B} d\vec{S} - \int_{A} \vec{C} d\vec{S} = \int_{A} S_T dA \quad (1)$$

Where, the control volume is represented with A and S is represented for the control surface, U is represented for the conservative variable and $\vec{C}$ and $\vec{B}$ are represented for diffusive and adjective fluxes. They are shown in Table 2.

Table 2-Navier-Stokes Equations variables

U	$\vec{B}$	$\vec{C}$
$\begin{bmatrix} \rho \\ \rho u \\ \rho v \\ \rho w \\ \rho E \end{bmatrix}$	$\begin{bmatrix} \rho v_i \\ \rho v_1 v_i + p\delta_{1i} \\ \rho v_2 v_i + p\delta_{2i} \\ \rho v_3 v_i + p\delta_{3i} \\ (\rho E + p) v_i \end{bmatrix}$	$\begin{bmatrix} 0 \\ \tau_{i1} \\ \tau_{i2} \\ \tau_{i3} \\ q_i + v_j \tau_{ij} \end{bmatrix}$

Where, tensor stress is represented with τ_{i1} as given in equation (2)

$$\tau_{i1} = \mu\left[\left(\frac{\partial v_j}{\partial x_i}\right) - \frac{2}{3}(\nabla. v)\delta_{ij}\right] \tag{2}$$

Where, i,j = 1,2,3.

2.3.2 Turbulence Models

In this work, SST k-w turbulence model which is two-equation models of Reynolds Averaged Navier-Stokes turbulence model was used for analyses.

SST k-ω turbulence model includes equations are generally: [7]

Turbulence kinetic energy,

$$\frac{\partial k}{\partial t} + U_j \frac{\partial k}{\partial x_j} = P_k - \beta^* k w + \frac{\partial k}{\partial x_j}\left[(v + \sigma_k v_T)\frac{\partial k}{\partial x_j}\right] \tag{3}$$

Specific Dissipation Rate,

$$\frac{\partial w}{\partial t} + U_j \frac{\partial k}{\partial x_j} = \alpha S^2 - \beta w^2 + \frac{\partial}{\partial x_j}\left[(v + \sigma_w v_T)\frac{\partial w}{\partial x_j}\right] + 2(1 - F_1)\sigma_{w2}\frac{1}{w}\frac{\partial k}{\partial x_i}\frac{\partial w}{\partial x_i} \tag{4}$$

Where, Blending Function (F1) is,

$$F_1 = \tanh\left\{\left\{min\left[max\left(\frac{\sqrt{k}}{\beta^* w y}, \frac{500v}{y^2 w}\right), \frac{4\sigma_{w2} k}{CD_{kw} y^2}\right]\right\}^4\right\} \tag{5}$$

$$CD_{kw} = \max\left(2\rho\sigma_{w2}\frac{1}{w}\frac{\partial k}{\partial x_i}\frac{\partial w}{\partial x_i}, 10^{-10}\right) \tag{6}$$

Kinetic eddy viscosity,

$$v_T = \frac{a_1 k}{\max\,(a_1 w, SF_2)} \tag{7}$$

$$F_2 = \tanh\left[\left[max\left(\frac{2\sqrt{k}}{\beta^* w y}, \frac{500v}{y^2 w}\right)\right]^2\right] \tag{8}$$

Production limiter (P_k),

$$P_k = \min\left(\tau_{ij}\frac{\partial U_i}{\partial x_j}, 10\beta^* k w\right) \tag{9}$$

2.4 Determining Formation Sequences

As a result of the aerodynamic analysis of single F-16 carried out in certain conditions, two different formation types were determined according to the number of aircrafts and contours showing the effect of the flow, and the analyses of these formation sequences were planned.

The analysis studies in this article were carried out only by determining the locations where the fighters in the formation sequence do not affect or low effect each other's airflows.

Depending on single F-16 aerodynamic analysis results, since the analyses are done at sea level, the air pressure is equal to 1atm. Therefore, the results show that the pressure borders represent the points where the absolute pressure is equal to 1atm. While determining the formations, the pressure borders play an important role for determining the field where the other fighters in the formation can be located with their own flow field. In this way, the areas where the fighters in the formation do not affect each other's flows or low effect were determined, and the formations were shaped in this direction.

Formation sequence for initial analysis:

Formation sequences were obtained interpreting the flow fields around the F-16. The free space that should be left in the vertical and horizontal distance between both F-16s is as shown in the Figure 7 and Figure 8. Also, *r* vector which is shown is in Figure 7 used for locating fighters for all formation types. Considering the *r* vector in this formation sequence, the formation was determined for an area where the flow was not disturbed according to the contours and analyses were made.

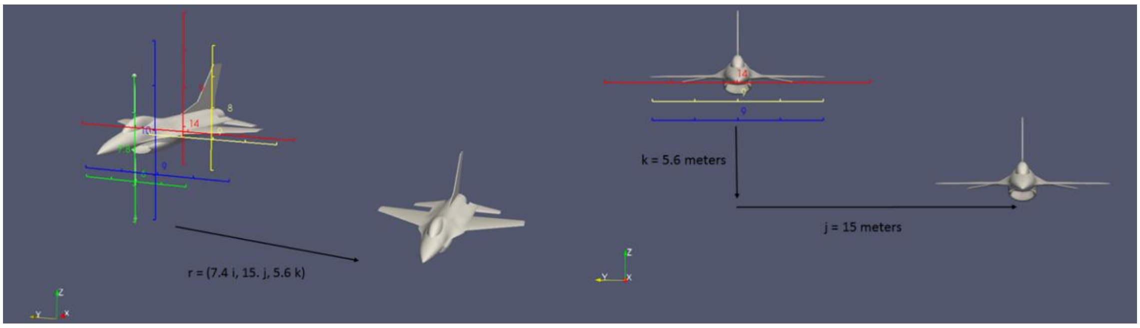

Figure 7-Formation for each two F-16 for vertical

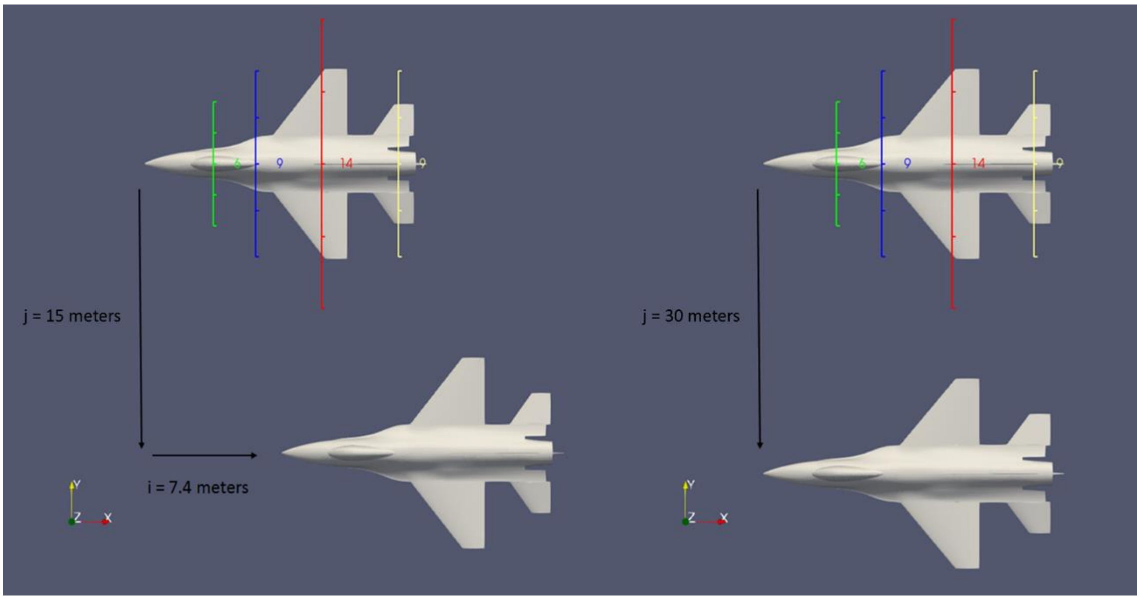

Figure 8-Formation for each two F-16 for horizontal

The vector of initial formation sequence was modified to represents large area.

For initial multiple F-16 formation sequences:

At the same altitude, for each two fighters:

$$r = (30\,j)$$

If there is an altitude differences, for each two fighters:

$$r = (7.4\,i, 15\,j, 5.6\,k)$$

According to *r* vector, for initial study, triple and quadruple formation sequences were formed as shown in Figure 9 and Figure 10 respectively.

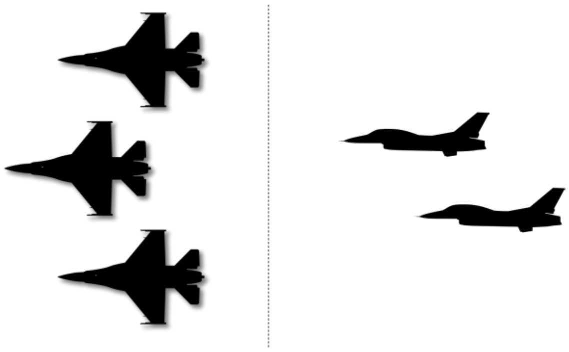

Figure 9-Illustration of initial triple F-16 formation sequence

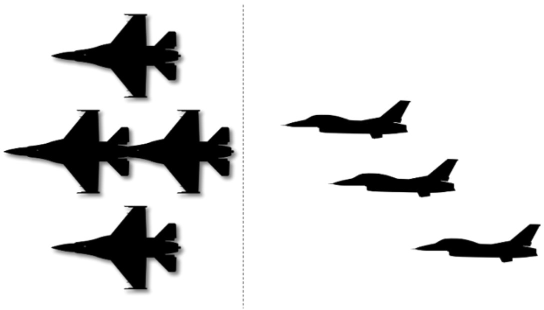

Figure 10-Illustration of initial quadruple F-16 formation sequence

Formation sequence for enhanced studies:

Formation sequences were obtained interpreting the flow fields around the F-16. The free space that should be left in the vertical and horizontal distance between both F-16s is as shown in the Figure 11 and Figure 13. Also, *r* vector which is shown is given at below used for locating fighters for all formation types. Studies were developed and the distances at the maximum points of the contours were determined for the minimum distance that the aircrafts can fly with being minimum affected by each other's air flow proper safe flight. The formation sequences were adjusted where made at the points where the effect of the flow is the least and the absolute air pressure is 1atm.

The vector of initial formation sequence was modified to represents large area.

For enhanced multiple F-16 formation sequences:

At the same altitude, for each two fighters:

$$r = (15\,j)$$

If there is an altitude differences, for each two fighters:

$$r = (7.4\,i, 7.5\,j, 5.6\,k)$$

According to *r* vector, for enhanced study, triple and quadruple formation sequences were formed as shown in Figure 12 and Figure 14 respectively.

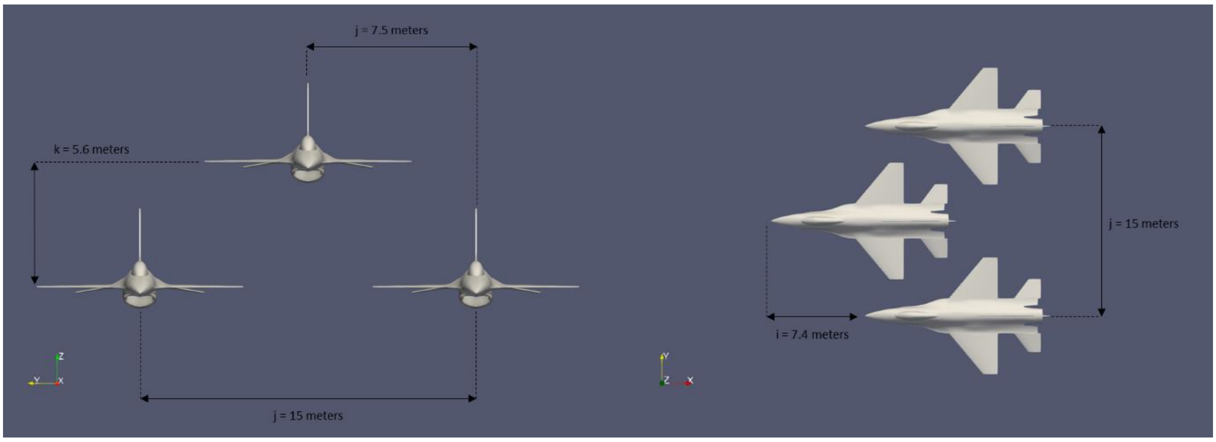

Figure 11-Enhanced formation of triple F-16

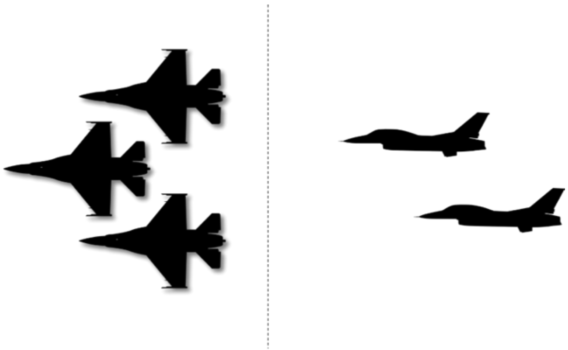

Figure 12-Illustration enhanced triple F-16 formation sequence

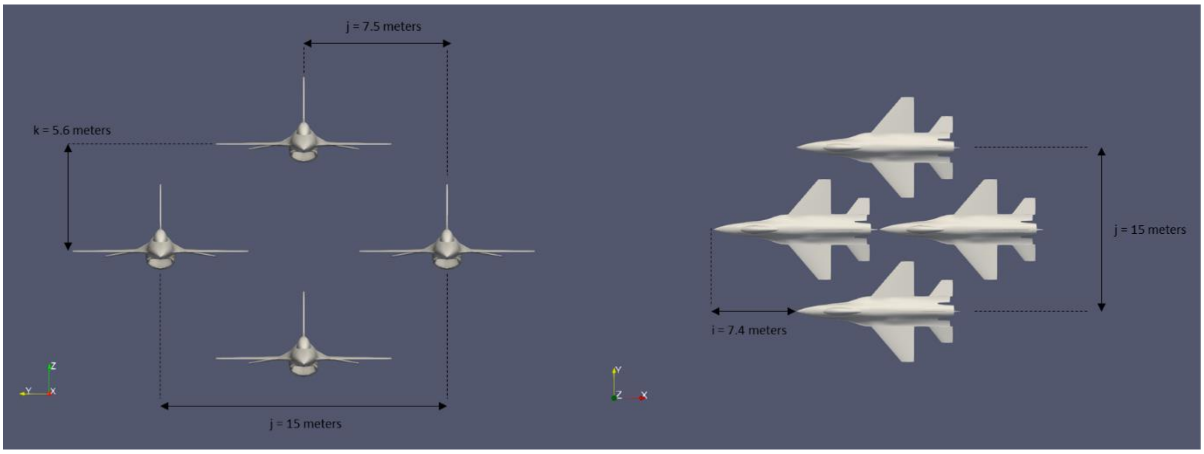

Figure 13-Enhanced formation of quadruple F-16

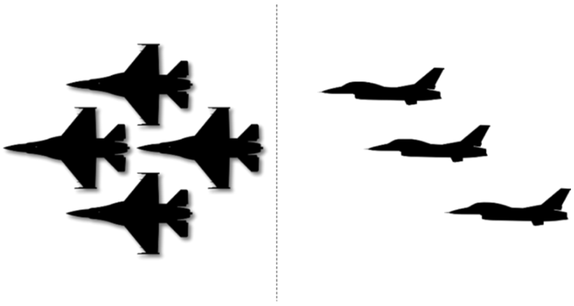

Figure 14-Illustration of enhanced quadruple F-16 formation sequence

Formation sequence rules were not formed only according to aerodynamic analysis results. One of the most important factors affecting the line-up is the pilot decisions.

As a result of the discussions with the F-16 test pilots, it was decided to form the formations within the limits below:

- The lead fighter must be within sight of the other aircraft in the formation. Also, the lead pilot should be able to see other fighters in close formation with a narrow viewing angle for safety.
- Close flight formations are suitable for flight in a formation where the lead pilot will communicate with the link and transfer situational awareness information to the other pilot over the main aircraft.
- Although flight formations to be carried out at close ranges at this level are not very suitable for sudden manoeuvres, they can be used for situations before the weapon launch, and this can increase the effectiveness in the tactical operational environment. The effect of the air flow over each aircraft on the other should be as minimal as possible.

2.5 CFD Analyses for Multi F-16 Formation Sequences

After single formation analyses are completed and verified multi F-16 formation analyses were made. Analyses were run on ANSYS Fluent at standard atmosphere sea level conditions with the freestream Mach Number of 0.9. The SST k-ω equations are used to model the turbulence. Computations have been done in a parallel computing environment using 40 processors on HPC (High Power Computing). A typical convergence history is given in Figure 15.

Figure 15-Residuals

2.6 Radar Detection Analysis

2.6.1 RCS (Radar Cross Section) Analysis Methods

The purpose of RCS analysis is to analyse how much the RCS changes compared a single F-16 to three and four F-16s in close formation flight. These results are the basis of analysis studies, supporting the study of the realism of the problem created by the close formation flights on the radar system. RCS value can change depending on radar system frequency, scanning angle of radar system, scattering points changes of target's geometry aspect with motion, polarization etc.

On the radar system of an aircraft, it is reflected on the pilot screen whether the enemy air elements are detected according to their RCS.

RCS calculation analysis was carried out under certain assumptions by positioning the triple F-16s shown in the Figure 16 at the relevant points and meshing these geometries with Pointwise.

RCS Calculation Formula is basically, [8]

$$\sigma(\phi) = \frac{\frac{power\ reflected\ source}{unit\ solid\ angle}}{incident\ power\ \frac{density}{4\pi}} = \lim_{R\to\infty} 4\pi R^2 \left|\frac{E^r}{E^i}\right|^2 \tag{10}$$

Where,

R=distance between the observation point and scatterer

E^r= reflected field strength of the observation point

E^i= strength of the incident field at the scattered

Φ= observation angle

Also, it can be defined as logarithmic quantity with respect to RCS,

$$\sigma_{dBsm} = 10\log_{10}\sigma/1m^2 \tag{11}$$

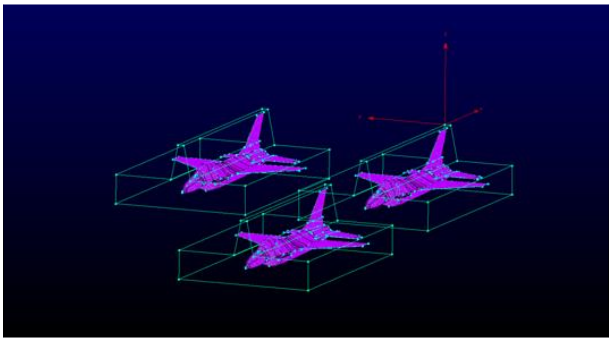

Figure 16-Meshed geometries in close flight formation position for RCS analysis

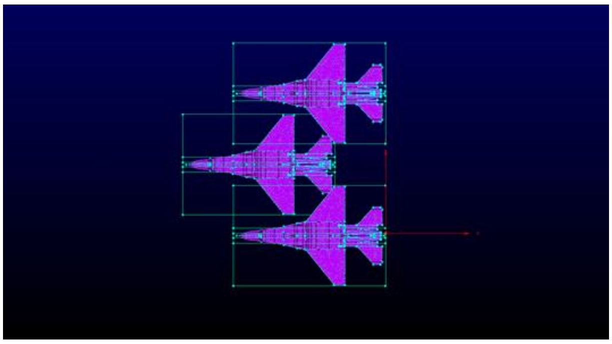

Figure 17-Meshed geometries in close flight formation position for RCS analysis-2

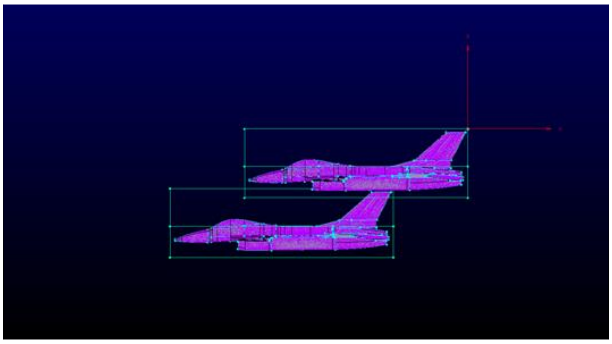

Figure 18-Meshed geometries in close flight formation position for RCS analysis-3

In Figure 16-17-18, as a sample, three F-16 Models positioned in close flight formation can be seen. RCS analysis was performed by applying mesh on these models. Also, RCS analysis were made for four F-16 formation type.

2.6.2 Probability of Detection Calculation

RCS is literally one of the Basic Radar Equation parameters and is used to calculate SNR (Signal to Noise Ratio) according to the capabilities of the radar system. [9]

$$SNR = \frac{P_S}{P_N} = \frac{P_T G_T G_R \sigma \lambda^2}{(4\pi)^3 k T_0 B F_n R^4 L} \tag{12}$$

where,

SNR= Signal to noise ratio

P_S= Signal power

P_N= Noise power

P_T= Transmitter power

G_T= Gain of the transmitter antenna

G_R= Gain of the receiver antenna

λ= Radar wavelength

σ= Target radar cross section

R= Range from the radar to the target

k= Boltzman's constant (1.38×10^{-23} w/(Hz°K)

T_0= Reference temperature

B= Effective noise bandwidth of the radar

F_n= Radar noise figure

L= Losses

The detection probability of the threat system is calculated with the P_d (Probability of Detection) formula at the bottom. [10]

$$P_d = 1 - \mathrm{erf}\left[\mathrm{erf}^{-1}\left(1 - P_{fa}\right) - SNR\right] \tag{13}$$

P_d= Probability of detection

P_{fa}= False alarm rate

3. Results

3.1 Aerodynamic Analysis Results

3.1.1 Single F-16 Analyses Results

CFD analyses were performed for the single F-16 under the assumptions mentioned in the methodology section with using ANSYS Fluent.

As a result of these analyses, the aoa value for the F-16 trim condition was determined as 0.565342°.

Figure 19 shows the pressure fields over a single F-16 while Figure 20 gives the supersonic regions. The maximum impact distances are shown in the Figure 21. These distances play an important role for formation sequences. These borders represent the maximum distances that can affect the airflows of the other aircraft in the formation sequence.

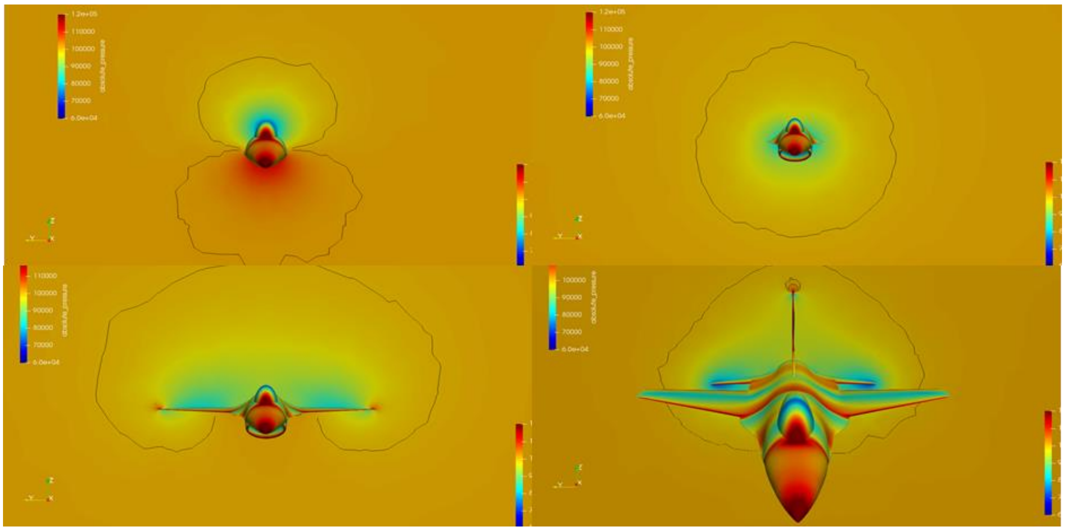

Figure 19-Pressure borders

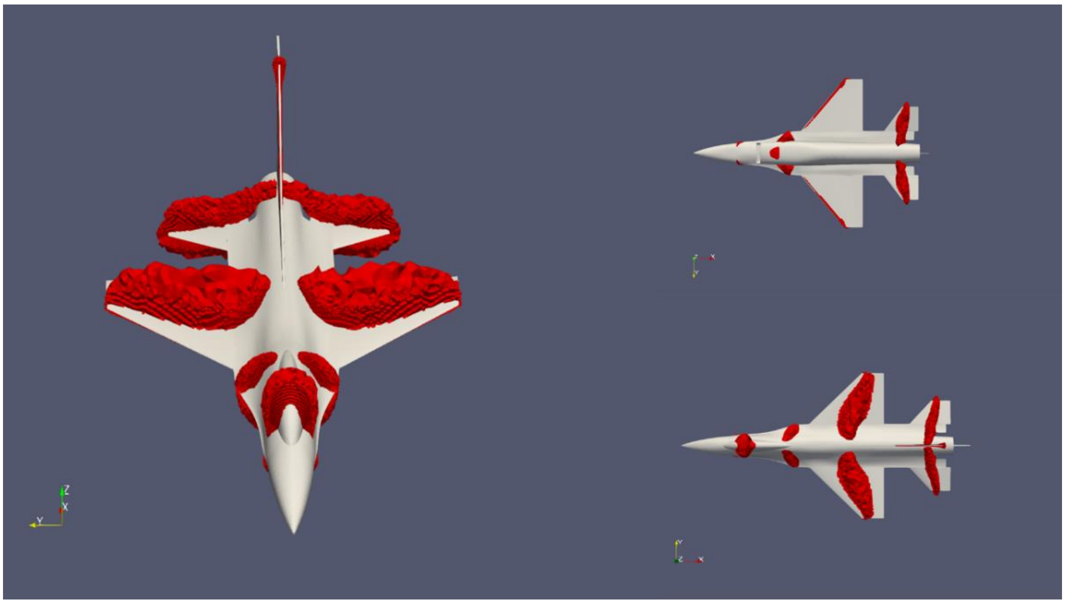

Figure 20-Points where flow is supersonic on F-16

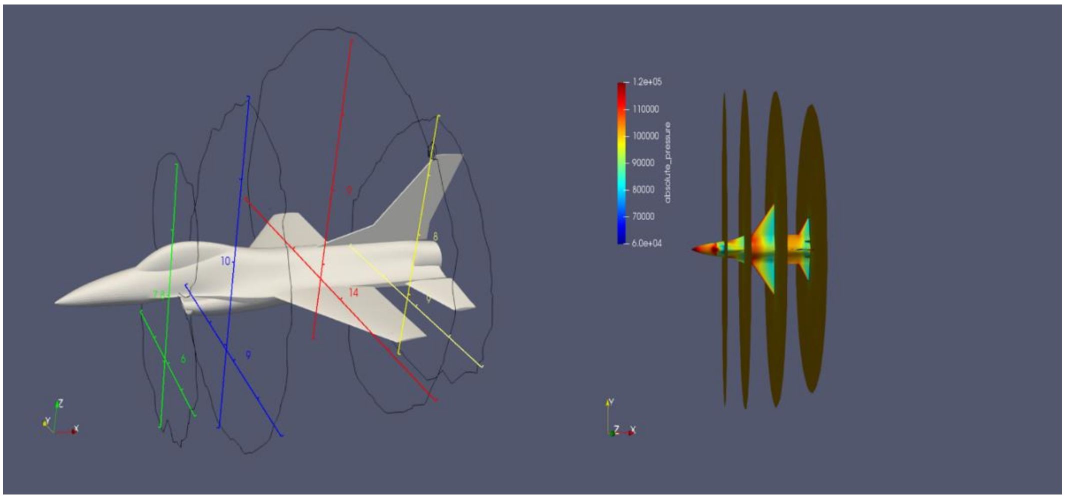

Figure 21-The dimensions of pressure borders and shock regions on body

3.1.2 Aerodynamic Analyses Results for Formation Sequences

After the formation positions were determined for each fighter, the flow fields around the F-16s flying in the multi-formation conditions were computed for initial analysis as mentioned in Section 2.4. Absolute pressure colour distribution on fighters' body in triple and quadruple formations are shown in Figure 22 and Figure 23 respectively.

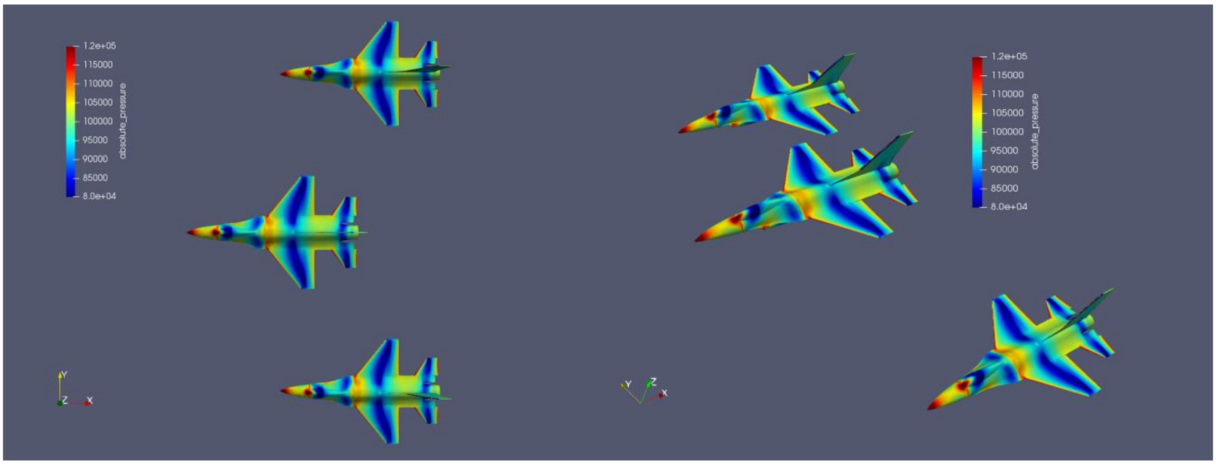

Figure 22-Absolute pressure colour distribution on initial triple F-16 formation type

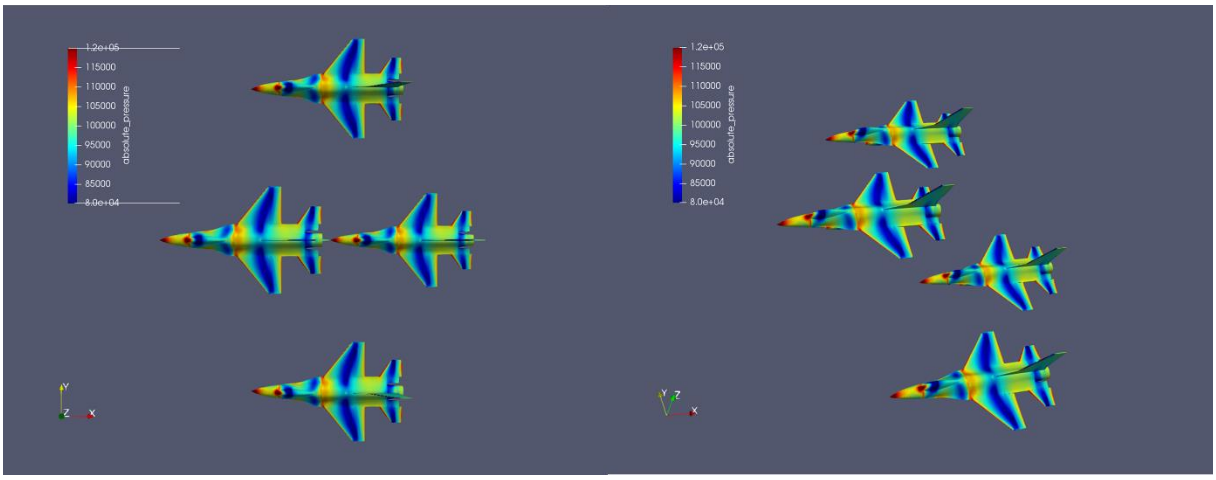

Figure 23-Absolute pressure colour distribution on initial quadruple F-16 formation type

Enhanced studies results, depending on new formation distances for triple and quadruple F-16 formation results as absolute pressure colour distributions on fighters body are shown in Figure 24 and Figure 25, respectively.

Table 3 includes C_D and C_L values for single F-16 and each fighter in initial formation sequences. C_L and C_D values for both the initial triple and quadruple formation sequences show very close values for each fighter in the formation sequences.

Table 3-Initial formation sequences C_L and C_D values

Formation Type	***Platform***	C_D	C_L
Single F-16		0.036	0.093
Triple F-16 Formation Sequence	Lead Fighter	0.037	0.095
	Crew 1	0.037	0.095
	Crew 2	0.037	0.095
Quadruple F-16 Formation Sequence	Lead Fighter	0.038	0.093
	Crew 1	0.038	0.093
	Crew 2	0.038	0.093
	Crew 3	0.038	0.093

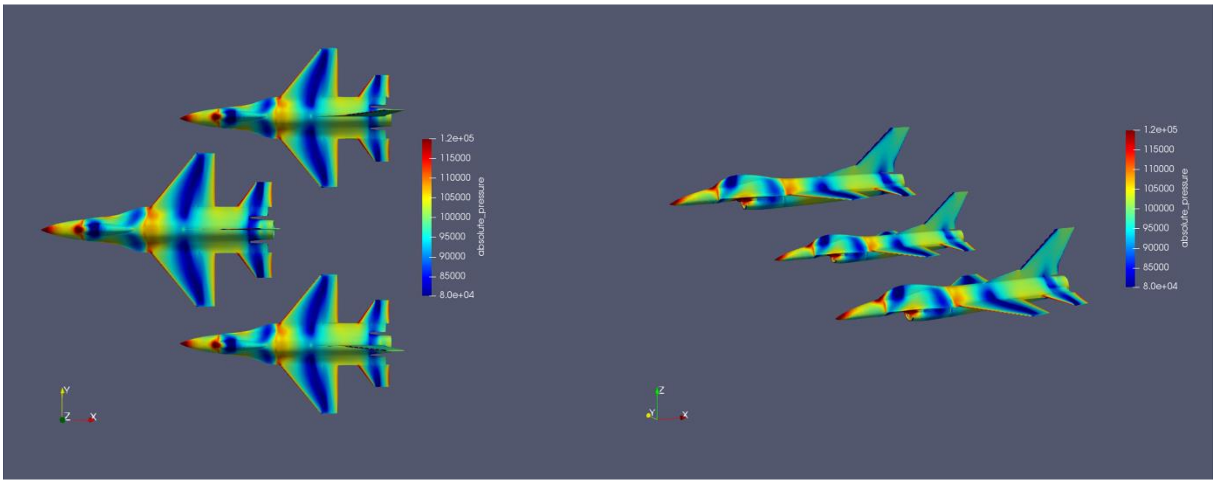

Figure 24-Absolute pressure colour distribution on enhanced studies triple F-16 formation type

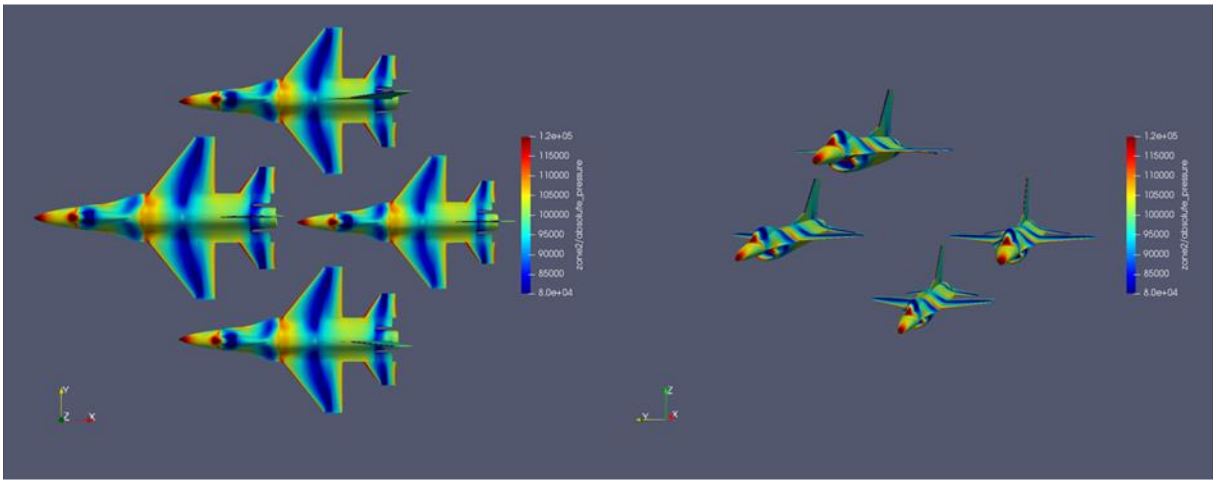

Figure 25-Absolute pressure colour distribution on enhanced studies quadruple F-16 formation type

Table 4 includes C_D and C_L values for single F-16 and each fighter in enhanced formation sequences. For both triple and quadruple enhanced formations, there is a small difference between C_D and C_L values which are suitable for safe flight in operational conditions for each F-16.

Table 4-Enhanced formation sequences C_L and C_D values

Formation Type	***Platform***	C_D	C_L
Single F-16		0.036	0.093
Triple F-16 Formation Sequence	Lead Fighter	0.037	0.108
	Crew 1	0.037	0.098
	Crew 2	0.037	0.098
Quadruple F-16 Formation Sequence	Lead Fighter	0.038	0.110
	Crew 1	0.037	0.104
	Crew 2	0.037	0.103
	Crew 3	0.036	0.097

3.2 RCS Results

The Analysis in this section were made to calculate the P_d value according to the RCS value of the threat system, which is considered for the BVR engagement starting distance, which is among the basic assumptions of our analysis.

For the formations, RCS calculation analyses were performed on POFACETS 4.1 [11] , which is open-source RCS analysis MATLAB based software. RCS calculation gives the results at below, regardless of the range, using the equation specified in the Section 2.6.1.

RCS value for single F-16 C: 1.2 m^2

RCS analysis for initial formations of triple and quadruple F-16 formation types:

RCS value of triple F-16s in close formation flights at 0° ≈ 63.1 m^2 (18 dBsm)

RCS value of quadruple F-16s in close formation flights at 0° ≈ 100 m^2 (20 dBsm)

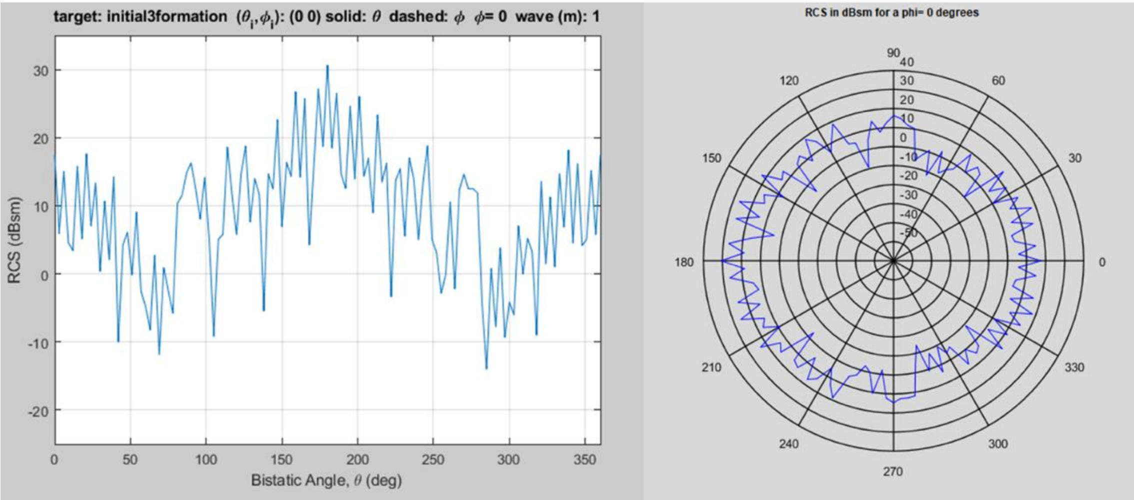

Figure 26-RCS Analysis results of triple F-16 formation for initial formations

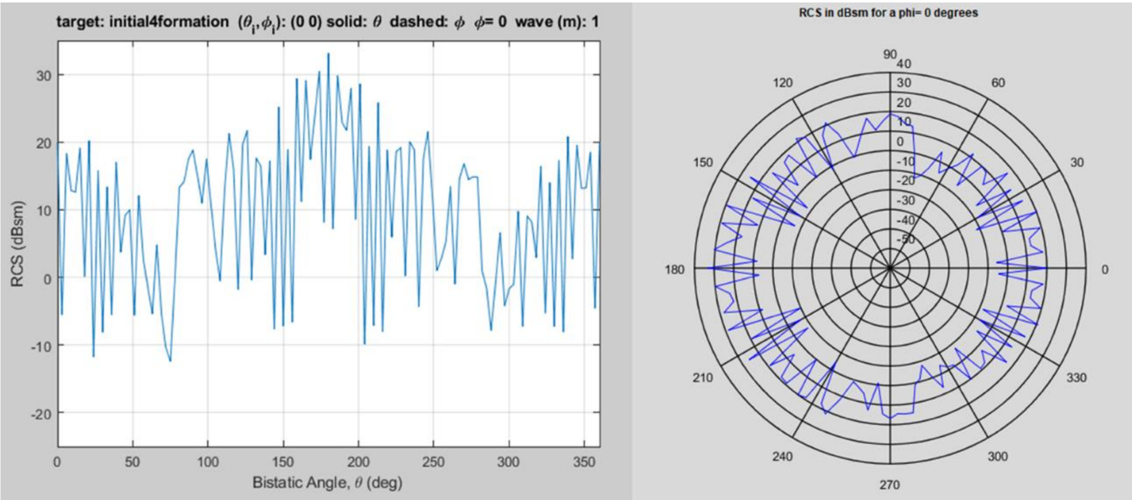

Figure 27-RCS Analysis results of quadruple F-16 formation for initial formations

RCS analysis for enhanced studies of triple and quadruple F-16 formation types:

RCS value of triple F-16s in close formation flights at 0° ≈ 50.1 m^2 (16.9 dBsm)

RCS value of quadruple F-16s in close formation flights at 0° ≈ 79.4 m^2 (19 dBsm)

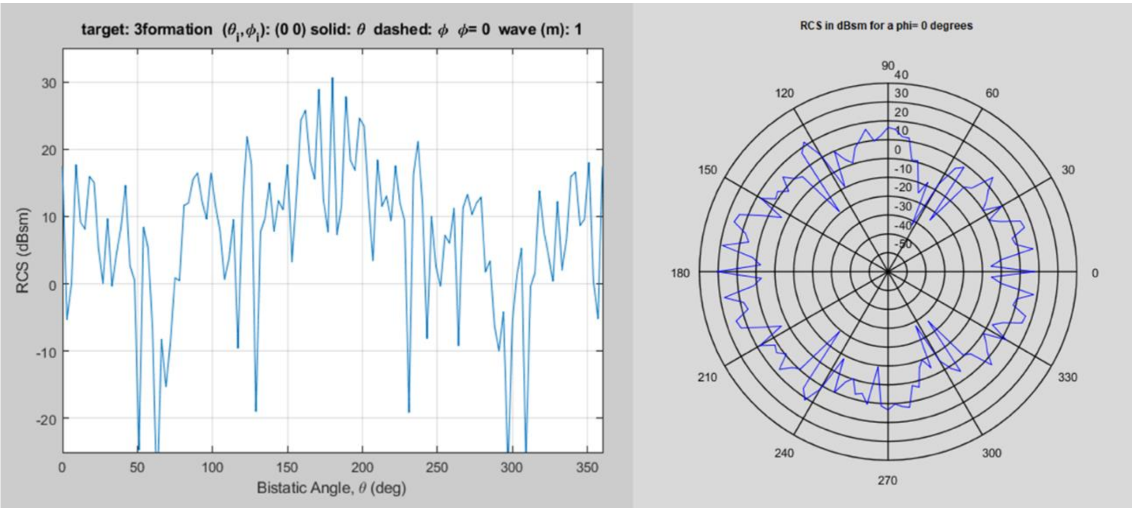

Figure 28-RCS Analysis results for triple F-16 formation for enhanced studies

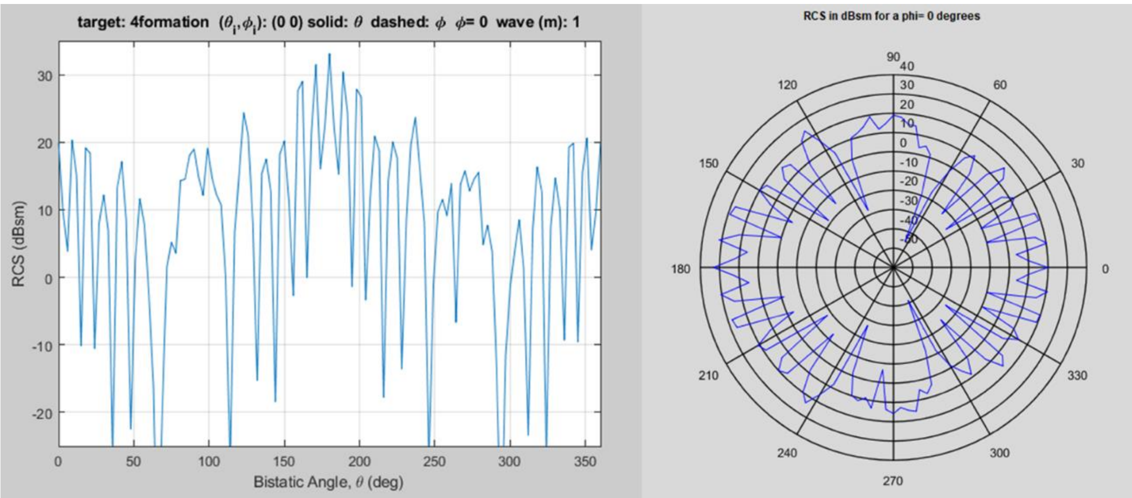

Figure 29-RCS Analysis results for quadruple F-16 formation for enhanced studies

In today's technologies, the most important features of 5th Generation Fighters are their low-observable capability. This generation of fighters, which can use its stealth feature as an advantage even at very high speeds, with its structural design and sensor capabilities, has a significant advantage against 4th and 4.5th generations. On the other hand, 5th generation aircrafts get a great advantage in the operational environment, not only against air threats but also against ground threats, with their low visibility features.

Based on these results, the RCS value of triple and quadruple F-16s in close flight formation is very close to the RCS value of an average large combat aircraft such as Military Transport Aircrafts or Bomber, according to open-source data. Based on this result, according to the problem that forms the basis of the analysis, triple and quadruple F-16s appear as a single large commercial or combat aircraft with a larger RCS value in the threat radar system. [12]

Table 5-RCS values of formation sequences compared with similar high RCS systems from literature

	RCS Analysis			Literature	
RCS Results	**Single F-16 (m^2)**	**Tripple F-16 Formation Sequence (m^2)**	**Quadruple Formation Sequence (m^2)**	**C-130 Hercules (m^2)**	**B-52 Stratofortress (m^2)**
Initial Studies	1.2	63.1	100	~80	~100
Enhanced Studies		50.1	79.4		

Figure 30 shows the formation sequences and the systems they approximately represent. Relevant close-flight formation sequences, F-16s in formation can be seen as similar high-RCS systems on the threat radar system.

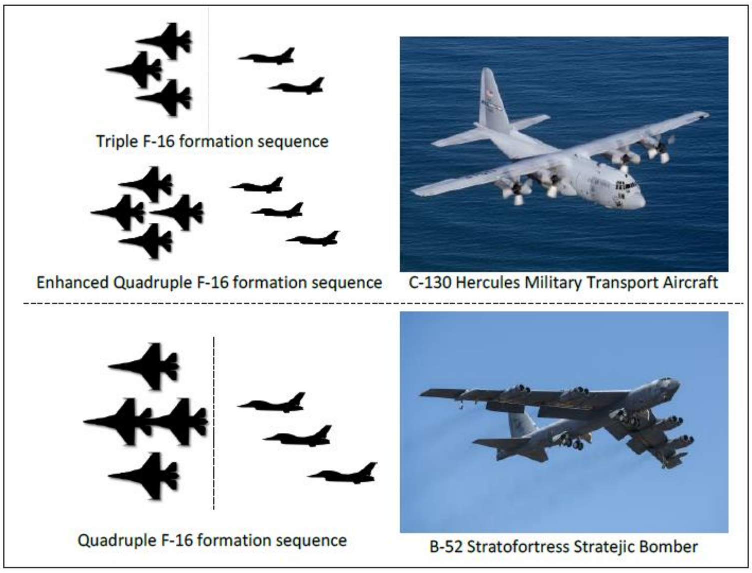

Figure 30-Comparison of formations depending on RCS results of formation sequences and representation in real-operational environment [13] [14]

3.3 Probability of Detection Analysis Result

After calculating the RCS values of the formation sequences, Pd versus Range curves were obtained using the methodology specified in Section 2.6.2. As seen in Figure 31, as the RCS value increases, the distance provided to the detection directly increases. For the enhanced study, which represents the formation sequences positions that were determined according to the new vector values determined, the RCS value decreases for the triple and quadruple formation arrays, and as a result, the distance at which they can be detected increases. Multiple formation arrays will be easier to detect on the radar system as the RCS value increases compared to a single F-16. This provides an advantage for formation arrays that aim to deceive the radar system.

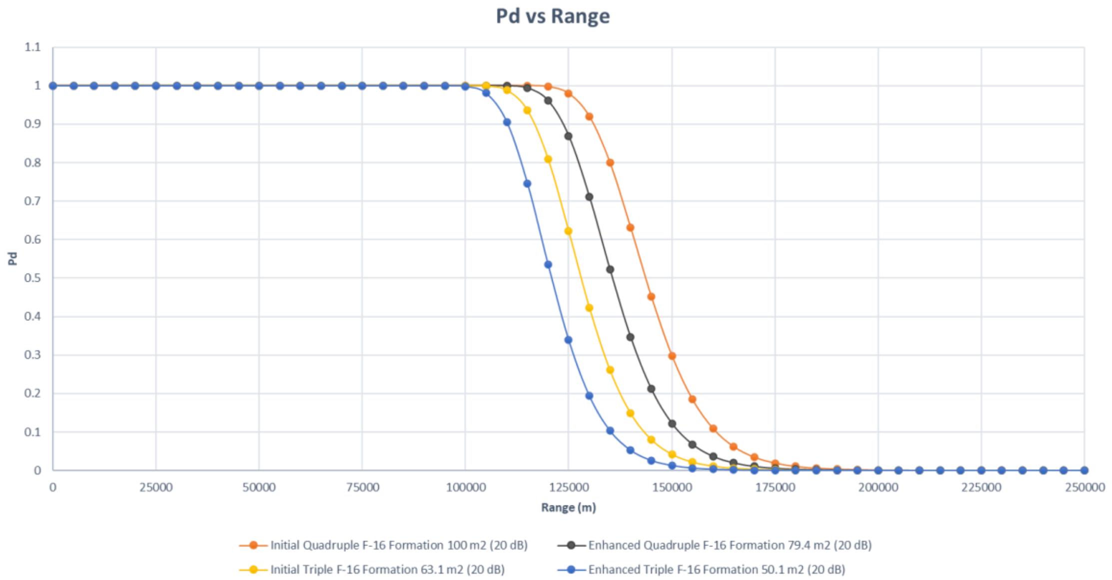

Figure 31-P_d versus Range curves for formation sequences

4. Conclusion

The RCS value read by the opposing system of three and four F-16s flying very close to each other seems like a value from a single aircraft, which is different from the F-16. The RCS values of the close flight formation types determined as a result of the analyses are similar to a single platform with high RCS values, such as very well-known commercial aircraft and military transport aircraft, considering the previous RCS calculation analyses in the literature.

It is observed that our proposed approach makes it difficult to distinguish targets in the Red Force radar system in close flight over Blue Force F-16s in formation flight. Since the radar system determines the classification on the threat system with the RCS value it sees on the system, the three and four F-16s, which cause a larger RCS value, now behave like a single system. Therefore, this will lead a challenging classification on the Red Force Radar System. Close flight formations increase the reflected RCS value but make it harder to target individually by threat systems. In an operational environment where 4th and 4.5th generation or lower generation fighters cannot use low observability capabilities because of structural limits, it is very important for success that it gains such a strong advantage, especially against 5th generation fighters, with a tactically innovative formation sequence.

In this way, within the scope of Blue Force subsystem capabilities, Fighters will now be able to approach the distance more easily where they can launch weapon against Red Force. This increases the *"Survivability"* factor for Blue Force by assuming that Red Force will reduce the probability of firing at each Blue Force F-16 performing close formation flight, and target lock performance will decrease. Similarly, within the scope of its own sub-system capabilities, the Blue Force can fire until it reaches the missile firing distance to the threat system in the far flight formation, with Red Force's superior system capabilities, and with using the new close flight formation, it gains the ability to reach this distance in a safer way and increase the *"Lethality"* factor as a result of gaining the ability of weapon launch.

These preliminary results show that the presented framework for the formation determination studies will help to increase the effectiveness of the old generation fighters in the operational environment. Tactical behaviours also vary according to the operational environment needs. As a future work, different formations will be examined with using similar methodologies and Mission Level scenarios will be reported for the determined formation methods, interpreted with the Operational Analysis perspective.

5. Contact Author Email Address

Please contact for any information with e-mail addresses of authors at below:

Süleyman Mert Aydın:
e-mail: 195114112@ybu.edu.tr
Company e-mail: suleymanmert.aydin@tai.com.tr
Personal e-mail: m.aydin650@gmail.com

Abdurrahman Gazi Yavuz:
e-mail: abdurrahmangazi.yavuz@tai.com.tr

Mustafa Kaya:
e-mail: mukaya@ybu.edu.tr

6. Copyright Statement

References

[1] Q. Zhang and H. H. Liu, “Aerodynamic Model-Based Robust Adaptive Control for Close Formation,” *Aerospace Science and Technology,* vol. 79, pp. 5-16, 2018.

[2] Z. Yu, Y. Zhang, B. Jiang, X. Yu, J. Fu, Y. Jin and T. Chai, “Distributed Adaptive Fault-Tolerence Close Formation Flight Control of Multiple Trailing Fixed-Wing UAV's,” *ISA Transactions,* vol. 106, pp. 181-199, 2020.

[3] Z. Yu, Y. Qu and Y. Zhang, “Safe Control of Trailing UAV in Close Formation Flight Against Actuator Fault and Wake Vortex Effect,” *Aerospace Science and Technology,* vol. 77, pp. 189-205, 2018.

[4] M. Gunasekaran and R. Mukherjee, “Aerodynamic Analysis of Wings in Chevron and V Formation Flight,” *European Journal of Mechanics - B/Fluids,* vol. 84, pp. 193-206, 2020.

[5] Z. A. Bangash, R. P. Sanchez, A. Ahmed and M. J. Khan, "Aerodynamics of Formation Flight," *Journal of Aircraft,* vol. 43, 2006.

[6] G. REDEKER, “A Selection of Experimental Test Cases for the Validation of CFD Codes,” Department of Commerce, Virginia, 1994.

[7] "SST K-Omega Turbulence Models," Autodesk, [Online]. Available: https://knowledge.autodesk.com/support/cfd/learn-explore/caas/CloudHelp/cloudhelp/2014/ENU/SimCFD/files/GUID-0F5C4828-9F91-46B6-A16A-2578D72DCFCC-htm.html. [Accessed 1 September 2022].

[8] R. Perez, “Radar Cross Section,” in *Wireless Communication Design Handbook,* California, Academic Press, 1999, p. 184.

[9] M. C. Budge, “Radar Range Equation,” 2011. [Online]. Available: http://www.ece.uah.edu/courses/materiaL/EE619-2011/RadarRangeEquation(2)2011.pdf. [Accessed 17 12 2021].

[10] R. Das and S. Singh, “Performance Modelling of Electro-Optical Devices for Military Target Acquisition,” *Defence Science Journal,* vol. III, no. 57, pp. 323-331, 2007.

[11] D. Jenn, “PROFACETS4.1,” 27 March 2012. [Online]. Available: https://www.mathworks.com/matlabcentral/fileexchange/35861-pofacets4-1?s_tid=mwa_osa_a. [Accessed 2022].

[12] K. Zikidis, A. Skondras and C. Tokas, “Radar Cross Section (RCS),” GlobalSecurity.org, [Online]. Available: https://www.globalsecurity.org/military/world/stealth-aircraft-rcs.htm. [Accessed 14 July 2022].

[13] L. M. C.-1. S. Hercules, Artist, *C-13 Hercules.* [Art]. Lockheed Martin C-130J Super Hercules, 1957.

[14] Boeing, Artist, *B-52 Stratofortress.* [Art]. Boeing, 1955.